Electronic Supplementary Information

Silver nanoparticles-decorated AlN whiskers hybrids for enhancing the thermal conductivity of nanofibrillated cellulose composite films

Mengyang Niu,[#a] Zheng Zhao, [#a] Baokai Wang,[a] Chang Yu,[a] Mengyi Li,[a] Jiajun Hu,[b] Ming Yue,[c] Qipeng Lu*[a] and Qi Wang*[a]

[a] *School of Materials Science and Engineering, University of Science and Technology Beijing, Beijing 100083, China.*

[b] *State Key Laboratory for Mechanical Behavior of Materials, Xi'an Jiaotong University, Xi'an, 710049, China.*

[c] *School of Civil and Resource Engineering, University of Science and Technology Beijing, Beijing 100083, China*

[#] Mengyang Niu and Zheng Zhao contributed equally to this work.

*Corresponding authors: qipeng@ustb.edu.cn (Q. Lu), wangqi15@ustb.edu.cn (Q. Wang)

Experimental Section

1. Chemicals

High-purity metallic iron powder (Fe) and aluminum particles (Al) were both procured from China Metallurgical Xindun Alloy. Nitrogen gas (N_2, 99.999%) and argon gas (Ar, 99.999%) were acquired from Tianjin Shengtang Gas. Anhydrous ethanol (CH_3CH_2OH, AR) was purchased from China National Pharmaceutical Group Chemical Reagent Beijing Co., Ltd. Polyvinylpyrrolidone (PVP, AR, average molecular weight 8000) and ascorbic acid ($C_6H_8O_6$, 99.99%) were obtained from Aladdin Reagent Co., Ltd. Silver nitrate ($AgNO_3$, AR) and 3-aminopropyltriethoxysilane (KH550) were sourced from Shanghai Trial of Traditional Chinese Medicine. A 1.2 wt% suspension of nanofibrillated cellulose (NFC) was procured from ScienceK.

2. Preparation of AlNw-AgNPs hybirds

The AlN whiskers were synthesized using a modified direct nitridation method, as reported in our previous literature.[1] After synthesis, the AlN whiskers were modified by KH550, which was developed as follows: KH550 was initially hydrolyzed in a mixture of anhydrous ethanol and water (volume ratio of 4:1) at 80 °C for 1 hour, ensuring 1wt% of KH550 was presented in the solution. A predetermined mass of AlNw, dispersed in anhydrous ethanol, was introduced into the fully hydrolyzed KH550 solution and continuously stirred at 80 °C for 2 hours. The resultant AlNw was collected via vacuum filtration, followed by drying in a thermostatic blast oven. Subsequently, 0.2 g of PVP was incorporated into 50 mL of deionized water. After 5

minutes of ultrasonication, 0.1 g of the modified AlNw was introduced, and magnetic stirring was applied for 30 minutes, followed by a further 30 minutes of ultrasonic dispersion. The suspension was gradually heated to 60 °C in a water bath, into which 2 ml of 0.01 mol/L $AgNO_3$ solution and 2 ml of 0.01 mol/L $C_6H_8O_6$ solution were successively dropwise added. The reaction was terminated after 5 minutes of constant stirring at 60 °C. The resulting solution was poured into a 45 ml centrifuge tube and separated at 5000 rpm for 5 minutes. The separated product was washed three times with anhydrous ethanol. Ultimately, the solid-phase product was collected and subsequently dried to yield the AlNw-AgNPs hybrids.

3. Preparation of NFC/AlNw Composite Films

The original NFC colloidal suspension was diluted in a beaker to obtain a suspension with a mass fraction of 0.1 wt%, followed by vigorous magnetic stirring for 2 hours. Subsequently, varying masses of ball-milled AlNw-AgNPs were introduced into the NFC suspension, followed by another 2 hours of intense magnetic stirring. The suspensions containing different AlNw-AgNPs mass fractions (0 wt%, 20 wt%, 40 wt%, 60 wt%, 70 wt%) were subjected to ultrasonic treatment for 30 minutes in an ultrasonic bath. Thereafter, using a circulating water vacuum pump in conjunction with a tangential flow filtration system, the NFC/AlNw suspension was subjected to vacuum filtration on a cellulose acetate filter membrane (pore size: 0.22 μm). Following the completion of the filtration process, the filtrate was placed in a thermostatic blast oven set at 60 °C for 24 hours, resulting in the final product of NFC/AlNw composite film with a thickness of several tens of micrometers.

4. Characterizations

The phase composition and crystalline structure of AlNw-AgNPs were characterized using a Rigaku Smartlab SE X-ray diffractometer (XRD) with Cu Kα radiation in the range of 10-90° (2θ). The microstructural morphology and structural characterization were performed using a Czech TESCAN MIRA LMS field emission scanning electron microscope (SEM) and a Japanese JEOL JEM-F200 transmission electron microscope (TEM). The SEM was equipped with an energy-dispersive X-ray spectroscopy (EDS) analyzer for elemental distribution analysis. An American Thermo Scientific Nicolet iS20 Fourier-transform infrared (FT-IR) spectrometer was employed to analyze surface functional groups before and after AlNw modification. The binding energies of different elements in the samples were characterized using an American Thermo Scientific ESCALAB 250Xi X-ray photoelectron spectroscopy (XPS) instrument. The in-plane and out-of-plane thermal diffusivity (α) of the composite film were tested at room temperature using the NETZSCH LFA 467 NanoFlash laser thermal analyzer. The average of at least three measurements was considered as the final result. The dimensions and shapes of the samples used for testing were as follows: circular with an in-plane diameter of 20 mm and square with dimensions of 10mm*10mm in the through-plane direction. The thermal conductivity (λ) of the samples was calculated using the following formula:

$$\lambda = \alpha \times \rho \times C_p \tag{1}$$

where ρ represented the density of the composite films, obtained through weighing and measuring dimensions, C_p represented the specific heat capacity of the composite films,

calculated using the blending rule, as shown by the following formula:

$$C_p = C_{\text{AlN-AgNPs}} \times \varphi + C_{\text{NFC}} \times (1 - \varphi) \quad (2)$$

where φ represented the volume fraction of fillers, and $C_{\text{AlN-AgNPs}}$ and C_{NFC} respectively stood for the room temperature specific heat capacities of AlNw-AgNPs and NFC, which were determined through Differential Scanning Calorimetry (DSC) using a TAQ600 instrument, yielding values of 0.51 $J \cdot g^{-1} \cdot K^{-1}$, 0.55 $J \cdot g^{-1} \cdot K^{-1}$, and 1.46 $J \cdot g^{-1} \cdot K^{-1}$ respectively. The volume resistivity of the composite film was measured using a Solartron electrochemical workstation, with samples of dimensions 5×10 mm. Conductive silver paste was applied to both ends as leads, and the current passing through the sample at a working voltage of 0.1 V was measured after clamping the leads with electrodes. The volume resistivity was then calculated based on the sample dimensions.

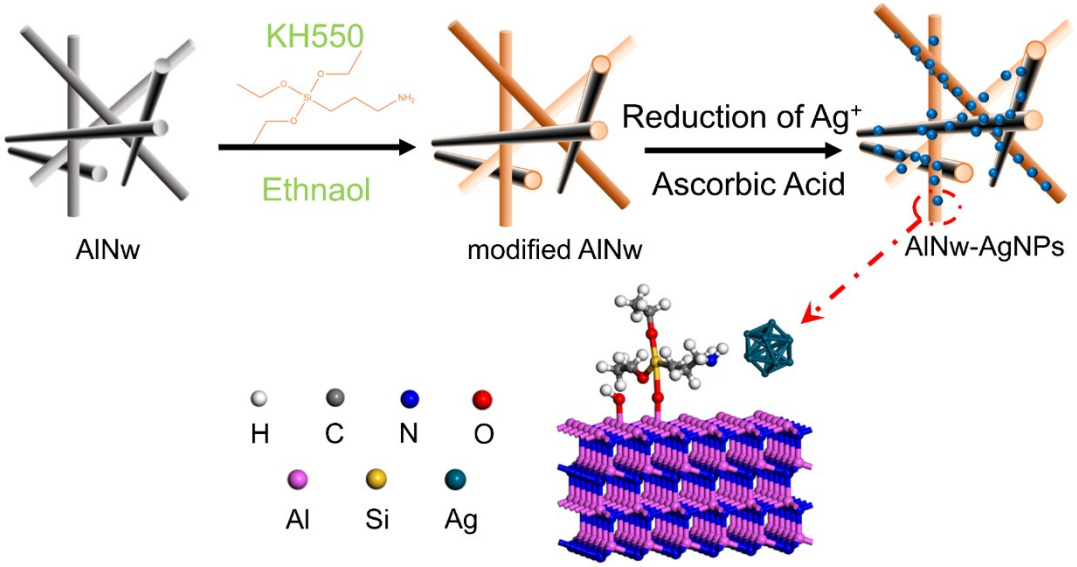

Figure S1. Schematic diagram of AlNw-AgNPs preparation process.

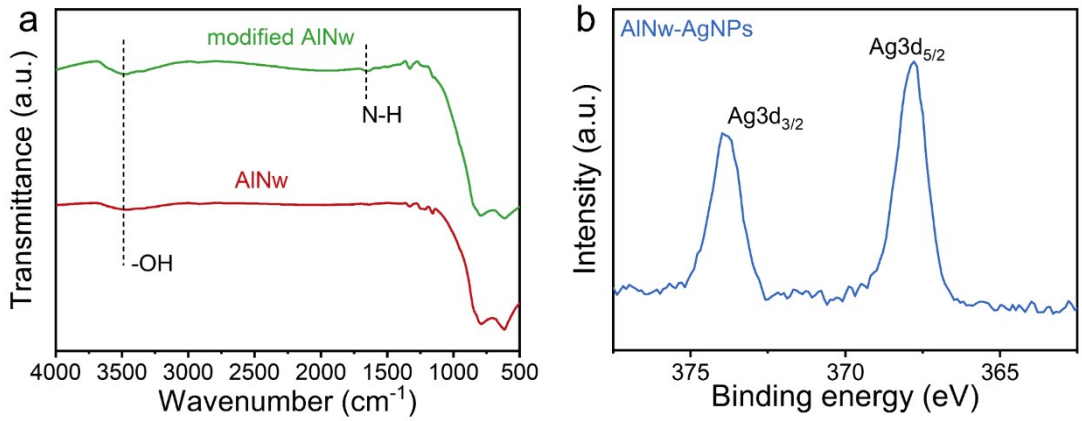

Figure S2. (a) FTIR spectra of AlNw before and after modification with KH550; (b) High-resolution XPS spectrum of Ag element in AlNw-AgNPs.

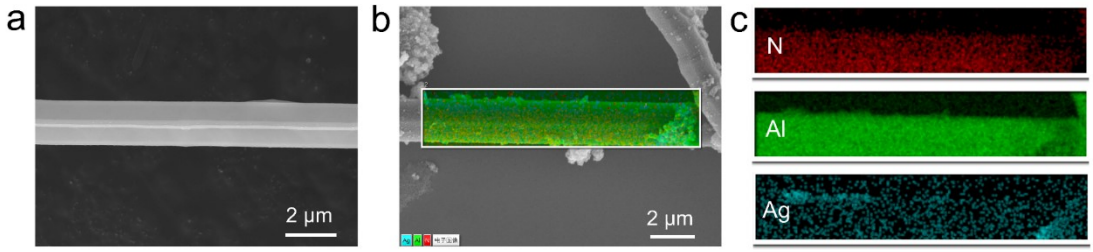

Figure S3. (a)SEM image of the as-synthesized AlNw, (b-c) EDS characterization of

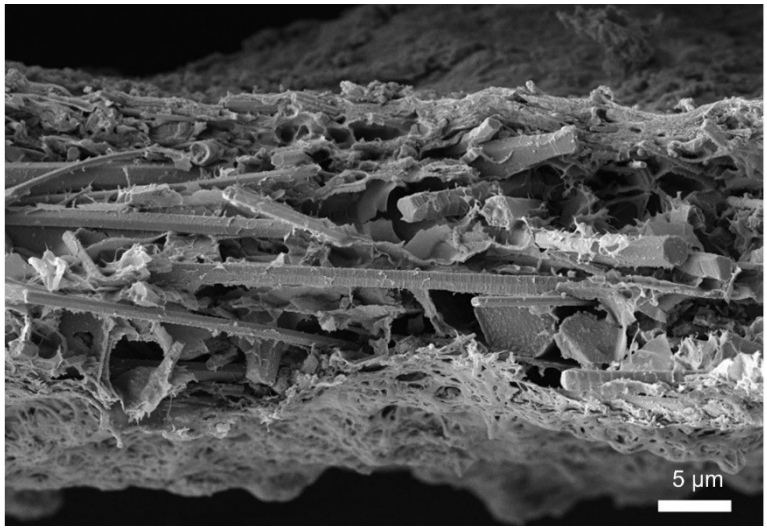

AlNw-AgNPs.

Figure S4. Cross-sectional SEM image of NFC/AlNw-AgNPs composite film with 70wt% filler content.

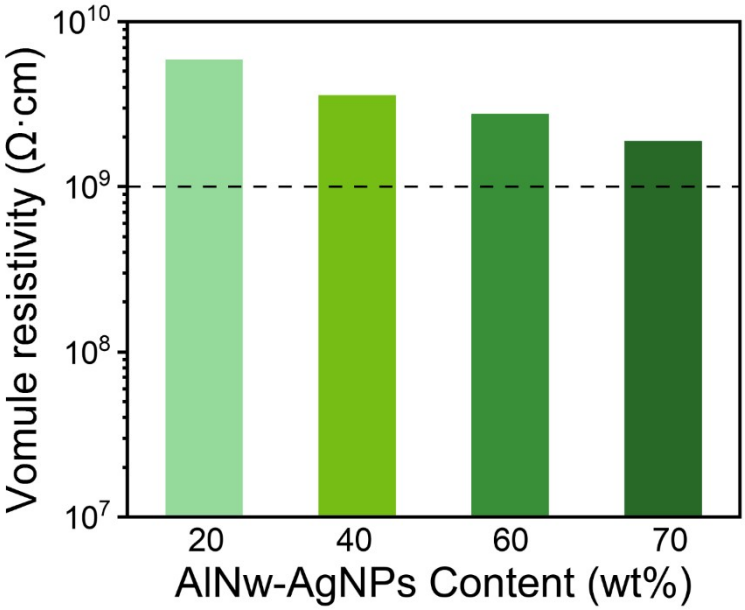

Figure S5. Volume resistivity of NFC/AlNw-AgNPs composite films with different AlNw-AgNPs contents.

Table S1. Comparison of in-plane thermal conductivity between NFC/AlNw-AgNPs composite film and some previously reported composite films.

Composites	Loading(wt%)	$\lambda_{/\!/}$(W/(m·K))	References
PVA/Si_3N_4NWs	50.0	15.40	[1]
NFC/AlN	25.0	4.20	[2]
PVDF/BNNS	33.0	16.3	[3]
NFC/MgO@rGO	20.0	7.45	[4]
CNC/BNNTS	20.0	13.33	[5]
NFC/MBP	15.0	17.60	[6]
PVA/FGN	80.0	21.60	[7]
PVA/SiCNWs	50.0	14.1	[8]
PVA/NF-BNNS	94.0	6.90	[9]
PVA/MWCNT-BN	20.0	11.49	[10]
CNF/H-MoS_2@SiCNWs	40.0	19.76	[11]
PVA/rGO	5.0	4.00	[12]
PMIA/AlN	50.0	17.30	[13]
NFC/AlNw-AgNPs	20.0	19.76	This work
NFC/AlNw-AgNPs	70.0	31.33	This work

Heat transfer simulation process for AlNw and AlNw-AgNPs models

Using the COMSOL Multiphysics 5.4 software, finite element simulations were employed to analyze the heat transfer processes of the AlNw and AlNw-AgNPs models. The heat source at the base of the AlNw heat transfer model was formulated as a rectangular prism with dimensions of 10×10×1 μm. The AlNw itself was approximated as a rod measuring 8μm in length and 0.5 μm in diameter. An array of 3×3 AlNw rods was uniformly distributed atop the heat source prism, with the lower surface of the AlNw rods in contact with the upper surface of the heat source prism. The heat transfer model for AlNw-AgNPs was constructed based upon the AlNw heat transfer model. On each surface of the AlNw rod, we introduced 48 uniformly distributed spherical models with a diameter of 80nm to represent the AgNPs. The remaining conditions were held consistent with those of the AlNw heat transfer model. Material properties were selected from the software's built-in material library. The bottom heat source prism was maintained at a fixed temperature of 473.15 K, while the initial temperature across the rest of the region was set to ambient temperature of 293.15 K. Grid generation was accomplished using an automated mesh partitioning technique, with grid sizes defined, followed by commencing the steady-state computation.

References

1 S. Wan, X. Hao, L. Zhu, C. Yu, M. Li, Z. Zhao, J. Kuang, M. Yue, Q. Lu, W. Cao and Q. Wang, *ACS Appl. Mater. Interfaces*, 2023, **15**, 32885-32894.

2 K. Zhang, P. Tao, Y. Zhang, X. Liao and S. Nie, *Carbohydr. Polym.*, 2019, **213**, 228-235.

3 J. Chen, X. Huang, B. Sun and P. Jiang, *ACS Nano*, 2019, **13**, 337-345.

4 M. Ma, L. Xu, L. Qiao, S. Chen, Y. Shi, H. He and X. Wang, *Chem. Eng. J.*, 2020, **392**, 123714.

5 Q. He, L. Ding, L. Wu, Z. Zhou, Y. Wang, T. Xu, N. Wang, K. Zhang, X. Wang, F. Ding, J. Zhang and Y. Yao, *Small Struct.*, 2023, **4**, 2200282.

6 J. Hu, H. Xia, X. Hou, T. Yang, K. Si, Y. Wang, L. Wang and Z. Shi, *J. Mater. Chem. A*, 2021, **9**, 27049-27060.

7 X. Chen, M. Wang, J. Cheng, C. Zhao and Z. Tang, *Mater. Today Chem.*, 2023, **29**, 101422.

8 Z. Chen, S. Gao, J. Zhang, D. Liu, J. Zeng, Y. Yao, J.-B. Xu and R. Sun, *Compos. Commun.*, 2023, **41**, 101654.

9 Z. Xiaoliang, Y. Lei, Y. Shuhui, L. Hao, S. Rong, X. Jianbin and W. Ching-Ping, *Nanoscale*, 2015, **7**, 6774-6781.

10 J. Zhou, Z. Yu, Y. Lv, C. Wang, P. Hu and Y. Liu, *Compos. Pt. A-Appl. Sci. Manuf.*, 2022, **163**, 107195.

11 B. Xue, S. Yang, X. Sun, L. Xie, S. Qin and Q. Zheng, *J. Mater. Chem. A*, 2020, **8**, 14506-14518.

12 F. Luo, M. Zhang, S. Chen, J. Xu, C. Ma and G. Chen, *Compos. Sci. Technol.*, 2021, **207**, 108707.

13 H. Ruan, F. Lü, J. Song, X. Bian, K. Yin, S. Yin and Q. Xie, *Compos. Sci. Technol.*, 2022, **224**, 109477.